Lázaro, M. (2019). Exact determination of critical damping in multiple exponential kernel-based viscoelastic single-degree-of-freedom systems. Mathematics and Mechanics of Solids. 24(12):3843-3861. https://doi.org/10.1177/1081286519858382

Exact determination of critical damping in multiple-exponential-kernel based viscoelastic single degree-of-freedom systems

Mario Lázaro[a,*]

[a] *Department of Continuum Mechanics and Theory of Structures*
Universitat Politècnica de València 46022 Valencia, Spain

Abstract

In this paper, exact closed-forms of critical damping manifolds for multiple-kernel based nonviscous single degree-of-freedom oscillators are derived. The dissipative forces are assumed to depend on the past history of the velocity response via hereditary exponential kernels. The damping model depends on several parameters, considered variables in the context of this paper. Those parameters combination which establish thresholds between induced overdamped and underdamped motion are called critical damping manifolds. If such manifolds are represented on a coordinate plane of two damping parameters, then they are named critical curves, so that overdamped regions are bounded by them. Analytical expressions of critical curves are deduced in parametric form, considering certain local nondimensional parameter based on the Laplace variable in the frequency domain. The definition of the new parameter (called critical parameter) is supported by several theoretical results. The proposed expressions are validated through numerical examples showing perfect fitting of the determined critical curves and overdamped regions.

Keywords:
Nonviscous damping, Critical damping, Critical parameter, Overdamped region, Critical curves, Critical surfaces, Viscoelastic damping, Exponential kernel

1. Introduction

In this paper, nonviscously damped single-degree-of-freedom oscillators are under study. Structures with nonviscous damping are made entirely or partially of so-called viscoelastic or time-dependent materials, used extensively in different areas of engineering mainly for vibration control and effective energy dissipation. These materials are characterized by hereditary behavior, i.e. the internal damping forces depend on the history of velocity response. Mathematically, hereditary effects are modeled using convolution integrals over kernel functions. Dynamic equilibrium of inertial, dissipative and stiffness forces on a single-degree-of-freedom system leads then to the integro-differential equation

$$m\ddot{u} + \int_{-\infty}^{t} \mathcal{G}(t-\tau)\,\dot{u}(\tau)\mathrm{d}\tau + k\,u(t) = f(t) \tag{1}$$

where $u(t)$ denotes the displacement, $f(t)$ the external applied force, k and m are the linear-elastic stiffness and mass, respectively. The time-dependent function $\mathcal{G}(t)$ represents the hereditary damping kernel. Fig. 1 shows the schematic configuration *mass-spring-viscoelastic damper* and the corresponding free body diagram.

It is implicitly assumed that the damping function $\mathcal{G}(t)$ satisfies the necessary conditions of Golla and Hughes [1] for a strictly dissipative behavior. As known, viscous damping can be considered just a particular case, expressed as $\mathcal{G}(t) \equiv c\,\delta(t)$, where c is the viscous damping coefficient and $\delta(t)$ is the Dirac's delta

*Corresponding author. Tel +34 963877000 (Ext. 76732). Fax +34 963877189
Email address: malana@mes.upv.es (Mario Lázaro)

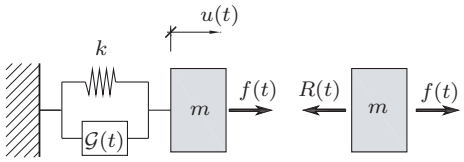

Figure 1: Left: a single degree-of-freedom viscoelastic oscillator with mass m, stiffness k and damping function $\mathcal{G}(t)$. Right: the free-body diagram with the external force applied $f(t)$ and the viscoelastic force reaction $R(t) = \int_{-\infty}^{t} \mathcal{G}(t-\tau)\,\dot{u}(\tau)\mathrm{d}\tau + k\,u(t)$

function. Checking solutions of the form $u(t) = e^{st}$ in Eq. (1) with $f(t) \equiv 0$, results in the characteristic equation in the s-domain (Laplace domain)

$$D(s) = m\,s^2 + s\,G(s) + k = 0 \tag{2}$$

where $G(s) = \mathcal{L}\{\mathcal{G}(t)\}$ is the Laplace transform of the damping function. There exists an extensive variety of viscoelastic models giving rise to different hereditary functions [2]. Among them, those that enable to express $G(s)$ in rational form are equivalent to the Biot's hereditary models [3] represented in time-domain as a finite series of exponential kernels. The characteristic equation (2) in the Laplace domain can be written in general as a polynomial of order $n = 2 + N$, where N is the number of exponential kernels within $G(s)$. The oscillatory nature of the roots (or eigenvalues) depends mainly on the mathematical form of the damping function in frequency domain, which in turn is governed by several damping parameters along with its dependence on s. The level of dissipation induced in the system is somehow controlled by these parameters because the eigenvalues implicitly depend on them through the relationship established in Eq. (2). Thus, eigenvalues of lightly damped systems will be formed by a conjugate-complex pair (with oscillatory nature) and N negative-real numbers called nonviscous eigenvalues [4, 5, 6] (these latter without oscillatory nature). Meanwhile, high damping can lead to a completely overdamped system in which all the $2 + N$ eigenvalues are negative-real numbers.

It makes sense to refer to critical damping in those viscoelastic models which are mathematically equivalent to a set of exponential hereditary kernels. Each kernel is associated to a nonviscous relaxation parameter and to a limit viscous coefficient. Hence, a multiple-kernel based model present several damping parameters, in particular $2N$ parameters for a N-kernels based model. Critical damping can be defined as that parameters combination which set the threshold between induced oscillatory and non-oscillatory motion. Consequently, the following geometrical structures can be considered: critical damping curves (when two damping parameters are under consideration), critical damping surfaces (for three parameters), or just critical manifolds (for more than three parameters). For exponentially damped oscillators based on a single kernel, the characteristic equation is equivalent to a third order polynomial. Muravyov [7] and Adhikari [8] derived its critical region through a rigorous study of the roots nature. A discussion about the oscillatory nature of the solutions an exponential viscoelastic oscillator is carried out by Müller [9]. With help of critical regions determined for exponentially damped oscillators, Adhikari [10] analyzed deeply the characteristics of the response in the frequency domain. Recently, Lázaro [11] has proved for nonviscous sytems that the critical manifolds arise from eliminating the parameter s from the two equations $D(s) = 0$ and $\partial D/\partial s = 0$. However, it is not trivial to address this task since the order of the polynomial increases at the same rate as the number of exponential kernels. As it is known, only analytical solutions for polynomials are available up to the fourth order. Hence, by this procedure, only critical regions for nonviscous models up to three kernels could be determined analytically. Even in the latter case, the radical based expressions (Cardano's formulas) needed to achieve closed forms of such critical surfaces can become extremely difficult to handle. This is probably the reason why such analytical forms of critical damping for oscillators with more than one exponential kernel have not been published yet. This leads to the fact that, at present, and as far as the author's knowledge goes, the only known closed-form critical region is still that of the single exponential kernel [7, 8].

The main contribution of this paper is to determine exact critical manifolds of multiple-kernel based nonviscous single degree-of-freedom oscillators. The key idea behind the approach is to consider such critical surfaces in parametric form instead of implicit functions, avoiding the problem of solving polynomials of high order. Necessary conditions to construct the mathematical expressions are provided in form of several theoretical results. The validation of the derived method is carried out through the numerical examples involving critical curves (in two parameters) and critical surfaces (in three parameters).

2. Theoretical background

Exponentially damped systems are based on the hypothesis that dissipative forces are depending on the time-history of velocity response via exponential kernel functions. The most general form of this model can be written as

$$\mathcal{G}(t) = \sum_{j=1}^{N} c_j \, \mu_j \, e^{-\mu_j t} \quad , \quad G(s) = \mathcal{L}\{\mathcal{G}(t)\} = \sum_{j=1}^{N} \frac{c_j \, \mu_j}{s + \mu_j} \tag{3}$$

where $\mu_j > 0$, $1 \leq j \leq N$ denote the relaxation or nonviscous coefficients, which govern the time and frequency dependence of the damping model. Parameters $c_j > 0$, $1 \leq j \leq N$ are the limit viscous coefficients, since they are related to the relaxation coefficients through

$$\sum_{j=1}^{N} c_j = \lim_{\mu_1 \ldots \mu_N \to \infty} G(s) = \int_0^\infty \mathcal{G}(t) \, dt \tag{4}$$

A proper choice of the parameters allows to identify the model given by (3) with any viscoelastic link formed by a finite number of springs and dampers [12]. For the purposes of this article, it is much more appropriate to present these variables in dimensionless form, defining

$$x = \frac{s}{\omega_n} \ , \quad \zeta_j = \frac{c_j}{2m\omega_n} \ , \quad \nu_j = \frac{\omega_n}{\mu_j} \tag{5}$$

where $\omega_n = \sqrt{k/m}$ is the undamped natural frequency, x denotes the nondimensional Laplace variable, ζ_j, ν_j , $1 \leq j \leq N$ represent respectively the jth viscous and nonviscous damping ratios, with range of validity $\zeta_j > 0$ and $\nu_j \geq 0$. In terms of the new variables, the damping function admits also a dimensionless form as

$$J(x) = \frac{G(x \, \omega_n)}{2m\omega_n} = \sum_{j=1}^{N} \frac{\zeta_j}{1 + x \, \nu_j} \tag{6}$$

and the characteristic equation (2) can now be rewritten as

$$\mathcal{D}(x) = \frac{D(x\omega_n)}{m\omega_n^2} = x^2 + 2 \, x \, J(x) + 1 = x^2 + 2 \sum_{j=1}^{N} \frac{x \, \zeta_j}{1 + x \, \nu_j} + 1 = 0 \tag{7}$$

This equation is equivalent to a polynomial of order $2 + N$, just multiplying $\mathcal{D}(x)$ by $\prod_{j=1}^{N}(1 + x\nu_j)$. In turn, Eq. (7) depends on $2N$ parameters, say

$$\boldsymbol{\theta} = (\zeta_1, \ldots, \zeta_N, \nu_1, \ldots, \nu_N) \tag{8}$$

The roots of equation $\mathcal{D}(x) = 0$ are then functions of the above $2N$ damping ratios, so that their oscillatory nature will depend on the value of the $2N$-tuple $\boldsymbol{\theta}$. It is suitable to introduce some definitions to facilitate understanding and notation.

Definition 1 (Damping Space)**.** *We call* Damping Space *to the following set*

$$\mathcal{H} = \{\boldsymbol{\theta} = (\zeta_1, \ldots, \zeta_N, \nu_1, \ldots, \nu_N) \in \mathbb{R}^{2N} : \zeta_j > 0 \, , \ \nu_j \geq 0 \ , \ 1 \leq j \leq N\} \tag{9}$$

Essentially, the damping space covers the validity range of the given damping ratios. In the damping space, each point will lie either on the overdamped or on the underdamped region. Both regions can be defined more rigorously as

Definition 2 (Overdamped and Underdamped Regions)**.** *Let*

$$\mathbf{x}(\boldsymbol{\theta}) = \{x_k(\boldsymbol{\theta})\}_{k=1}^{2+N}$$

be the array formed by the $2+N$ *roots of the Eq.* (7) *for certain point* $\boldsymbol{\theta} \in \mathcal{H}$*. We define the following subsets within the damping space*

(i) The Overdamped Region *is the subset of* $\mathcal{H}$ *which induces a completely overcritical response with all eigenvalues negative real numbers, namely*

$$\mathcal{OD} = \{\boldsymbol{\theta} \in \mathcal{H} : \Im(\mathbf{x}(\boldsymbol{\theta})) = \mathbf{0}\}$$

(ii) The Underdamped Region *is the subset of* $\mathcal{H}$ *which induces an oscillatory response: two eigenvalues of the set* $\mathbf{x}(\boldsymbol{\theta})$ *form a conjugate-complex pair. Mathematically, it can be expressed as*

$$\mathcal{UD} = \{\boldsymbol{\theta} \in \mathcal{H} : \Im(\mathbf{x}(\boldsymbol{\theta})) \neq \mathbf{0}\}$$

In the above definitions, $\Im(\bullet)$ denotes the imaginary part. Those thresholds separating underdamped and overdamped regions define the critical manifolds. However, a mathematical characterization of the critical manifold can be given using a previous result

Definition 3 (Lázaro [11])**.** *The* Critical Manifold *of a single-degree-of-freedom oscillator is the subset of points* $\boldsymbol{\theta} \in \mathcal{H}$ *characterized by*

$$\mathcal{C} = \{\boldsymbol{\theta} \in \mathcal{H} : \exists!\ x_c \in \mathbf{x}(\boldsymbol{\theta})\ /\ \mathcal{D}(x_c) = 0 \text{ and } \mathcal{D}'(x_c) = 0\}$$

where x_c *denotes the critical eigenvalue associated to* $\boldsymbol{\theta}$ *and* $(\bullet)' = \partial(\bullet)/\partial x$*.*

Strictly, the critical manifold is a subset of the overdamped region, but geometrically constitutes a $(2N-1)$-dimensional manifold characterized by the fact that one of the roots is double. Furthermore, if certain $\boldsymbol{\theta} \in \mathcal{H}$ lies in the critical manifold, one and only one eigenvalue within $\mathbf{x}(\boldsymbol{\theta})$ will be double, since it cannot be double nonviscous eigenvalues [5].

Here is a simple example to enlighten the concepts introduced above. Let us consider for instance the case $N = 2$, with two exponential kernels. The damping space is then the 4-dimensional domain

$$\mathcal{H} = \{(\zeta_1, \zeta_2, \nu_1, \nu_2) \in \mathbb{R}^4 : \zeta_1, \zeta_2 > 0\,,\ \nu_1, \nu_2 \geq 0\ ,\ 1 \leq j \leq N\} \tag{10}$$

and critical regions are 3-dimensional manifolds with the form

$$f(\zeta_1, \zeta_2, \nu_1, \nu_2) = 0$$

which are equivalent to critical volumes, from a geometrical point of view. Cross sections to this volume, for example by certain value $\nu_2 = \nu_{20}$, give rise to 2-dimensional manifolds (or critical surfaces) with equation

$$g(\zeta_1, \zeta_2, \nu_1) = f(\zeta_1, \zeta_2, \nu_1, \nu_{20}) = 0$$

which can be visualized in the subspace $(\zeta_1, \zeta_2, \nu_1) \in \mathbb{R}^3$. Furthermore, cross sections to the above surface, for instance $\nu_1 = \nu_{10}$, leads now to 1-dimensional manifolds (or critical curves)

$$h(\zeta_1, \zeta_2) = f(\zeta_1, \zeta_2, \nu_{10}, \nu_{20}) = 0$$

which can be plotted in the plane (ζ_1, ζ_2).

The above representation of critical regions in implicit form has been written theoretically. That would be available if the variable x could be solved as an explicit function of the damping parameters from one of the two equations

$$\mathcal{D}(x) = 0 \ , \quad \mathcal{D}'(x) = 0 \tag{11}$$

and plugged into the other one, something that becomes only possible for $N \leq 3$. Indeed, in such case, $\mathcal{D}(x)$ can be reduced to a 5th order polynomial, then $\mathcal{D}'(x)$ is of 4th order and the Cardano-Ferrari's formulas could theoretically be used. However, the complexity of radicals-based expressions would make unapproachable in practice the attempt of finding interpretable results. Thus, instead of addressing the problem considering x as an unknown to be eliminated, our approach assumes that x is a parameter itself. The following result allows to predict the range of validity of any critical eigenvalue.

Theorem 1. *If $x = s/\omega_n \in \mathbb{R}^-$ is a (nondimensional) critical eigenvalue, then*

(i) $x \leq -1$

(ii) $x = -1$ *if and only if* $\sum_{j=1}^{N} \zeta_j = 1$ *and* $\nu_j = 0,\ 1 \leq j \leq N$

Proof. (i) If $x \in \mathbb{R}^-$ is a critical eigenvalue, then according to the Definition 3, the following equations hold simultaneously

$$\mathcal{D}(x) = x^2 + 2xJ(x) + 1 = 0 \tag{12}$$
$$\mathcal{D}'(x) = 2\left[x + J(x) + xJ'(x)\right] = 0 \tag{13}$$

Eliminating $J(x)$ from both equations and simplifying, it yields

$$x^2\left[1 + 2J'(x)\right] = 1 \tag{14}$$

Rearranging the terms of the equation

$$x^2 - 1 = -2\,x^2\,J'(x) = \sum_{j=1}^{N} \frac{2\,x^2\,\zeta_j\,\nu_j}{(1 + x\,\nu_j)^2} \geq 0 \tag{15}$$

The right part of the equation is non-negative, therefore necessarily it is $x^2 \geq 1$. Thus, since $x < 0$, the critical eigenvalue verifies $x \leq -1$

(ii) Let us assume first that $s = -\omega_n$, that is $x = -1$ in nondimensional form. Plugging into Eqs. (12) and (13) yields

$$\mathcal{D}(-1) = 1 - 2J(-1) + 1 = 0 \tag{16}$$
$$\mathcal{D}'(-1) = 2\left[-1 + J(-1) - J'(-1)\right] = 0 \tag{17}$$

From the two equalities, it follows that $J(-1) = 1$ and $J'(-1) = 0$. Written both expressions as functions of the damping parameters, we have

$$J(-1) = \sum_{j=1}^{N} \frac{\zeta_j}{1 - \nu_j} = 1 \tag{18}$$

$$J'(-1) = -\sum_{j=1}^{N} \frac{\zeta_j\,\nu_j}{(1 - \nu_j)^2} = 0 \tag{19}$$

By hypothesis we have that $\zeta_j > 0$, $\nu_j \geq 0$. Therefore, from Eq. (19) it necessarily yields $\nu_j = 0\ ,\ 1 \leq j \leq N$. Finally, plugging these latter expressions into Eq. (18), it results $\sum_j \zeta_j = 1$. The reciprocal statement is straightforward since the assumptions $\sum_j \zeta_j = 1$ and $\nu_j = 0\ , \forall j$ lead the system to the purely viscous state, with characteristic equation $(x + 1)^2 = 0$. □

Remark: Eq. (15) is valid not only for strictly exponentially damped systems but for any viscoelastic oscillator with a damping function in the time domain holding $\mathcal{G}(t) \geq 0,\ \forall t \geq 0$. Indeed, using the definition of the s-derivative of a Laplace transform, it yields

$$J'(x) = \frac{1}{2m}\ \left.\frac{\partial G}{\partial s}\right|_{s=x\omega_n} = -\frac{1}{2m}\,\mathcal{L}\{t\,\mathcal{G}(t)\}_{s=x\omega_n} \leq 0 \tag{20}$$

Hence it follows that potential non-exponential viscoelastic models also verify the relationship (15) and the methodology developed in this paper could also be applied on them.

Theorem 1 turns out to be key for the purposes of this article, showing that any critical eigenvalue will lie inside the interval $-\infty < x \leq -1$. This means that its inverse in absolute value, $1/|x|$, is bounded by 0 and 1, something that leads to the following definition

Definition 4 (Critical parameter, α)**.** *Assume $x \in \mathbb{R}^-,\ -\infty < x \leq -1$ is a critical eigenvalue, then the* critical parameter α *associated to x is defined as*

$$\alpha = -\frac{1}{x}\ \in (0,1]$$

This new definition enables construction of critical curves in parametric form, something that will be developed in the next Section.

3. Exact determination of critical damping

From the theoretical results given in Theorem 1 and Definition 4, both equations, $\mathcal{D}(x) = 0$ and $\mathcal{D}'(x) = 0$, can be observed from other point of view. Instead of considering x as an unknown, it can be interpreted as an independent variable written in terms of the above defined *critical parameter*, α, which varies in the finite interval $0 < \alpha \leq 1$. Plugging the relationship $x = -1/\alpha$ into Eqs (12) and (13), it yields

$$\mathcal{D}(-1/\alpha) \;=\; \frac{1}{\alpha^2} - \frac{2}{\alpha}\sum_{j=1}^{N}\frac{\zeta_j}{1-\nu_j/\alpha} + 1 = 0 \tag{21}$$

$$\left.\frac{\partial \mathcal{D}}{\partial x}\right|_{x=-1/\alpha} \;=\; -\frac{1}{\alpha} + \sum_{j=1}^{N}\frac{\zeta_j}{1-\nu_j/\alpha} - \frac{1}{\alpha}\sum_{j=1}^{N}\frac{\zeta_j\nu_j}{(1-\nu_j/\alpha)^2} = 0 \tag{22}$$

After some straight simplifications, both equations can be expressed as

$$\sum_{j=1}^{N} R_j(\alpha)\,\zeta_j \;=\; \frac{\alpha^2+1}{2\alpha} \tag{23}$$

$$\sum_{j=1}^{N} R_j^2(\alpha)\,\zeta_j \;=\; \frac{1}{\alpha} \tag{24}$$

where $R_j(\alpha),\ 1 \leq j \leq N$, defined as

$$R_j(\alpha) = \frac{\alpha}{\alpha - \nu_j} \tag{25}$$

are auxiliary functions of the nonviscous damping ratios ν_j and the critical parameter α. Eqs. (23) and (24) can easily be solved in terms of any pair of unknowns within the set $\{\zeta_1, \ldots, \zeta_N, \nu_1, \ldots, \nu_N\}$. For instance, let us assume that we are interested in graphing the critical curve relating the viscous ratios ζ_i and ζ_k, $i \neq k$, considering fixed the rest of $2N-2$ damping parameters. Eqs. (23) and (24) can be rewritten as

$$\zeta_i\,R_i(\alpha) + \zeta_k\,R_k(\alpha) \;=\; U_{ik}(\alpha) \tag{26}$$

$$\zeta_i\,R_i^2(\alpha) + \zeta_k\,R_k^2(\alpha) \;=\; V_{ik}(\alpha) \tag{27}$$

where

$$U_{ik}(\alpha) = \frac{\alpha^2+1}{2\alpha} - \sum_{\substack{j=1 \\ j\neq\{i,k\}}}^{N} R_j(\alpha)\,\zeta_j \tag{28}$$

$$V_{ik}(\alpha) = \frac{1}{\alpha} - \sum_{\substack{j=1 \\ j\neq\{i,k\}}}^{N} R_j^2(\alpha)\,\zeta_j \tag{29}$$

Determination of ζ_i and ζ_k is then straightforward, yielding

$$\zeta_i(\alpha) = \frac{R_k(\alpha)\,U_{ik}(\alpha) - V_{ik}(\alpha)}{R_i(\alpha)\,[R_k(\alpha) - R_i(\alpha)]} \quad , \quad 0 < \alpha \leq 1 \tag{30}$$

$$\zeta_k(\alpha) = \frac{R_i(\alpha)\,U_{ik}(\alpha) - V_{ik}(\alpha)}{R_k(\alpha)\,[R_i(\alpha) - R_k(\alpha)]} \quad , \quad 0 < \alpha \leq 1 \tag{31}$$

The above equations represent the critical curve in parametric form. Its graph $\{(\zeta_i(\alpha), \zeta_k(\alpha)),\ 0 < \alpha \leq 1\}$ can be drawn in the coordinate plane formed by axes (ζ_i, ζ_k) and it emerges from the evaluation of the above expressions in the interval $0 < \alpha \leq 1$. If one of the fixed damping parameters, say ζ_l, is assumed to be variable in certain interval I, then the family of critical curves

$$\{(\zeta_i(\alpha,\beta), \zeta_k(\alpha,\beta), \beta)\,,\ 0 < \alpha \leq 1\,,\ \beta \in I\} \tag{32}$$

represent a 2-dimensional manifold in the 3D coordinate axes $(\zeta_i, \zeta_k, \zeta_l)$, i.e. a critical surface. The total amount of different critical curves arises from the combination of the total number of viscous and nonviscous damping ratios $(2N)$ taken by pairs, that is $\binom{2N}{2} = N(2N-1)$ curves. However, due to the symmetry of the problem respect to ζ_j and ν_j $1 \leq j \leq N$, such amount can be reduced just to the following 4 types:

Type I. Critical curves that relate pairs of different viscous ratios $\{\zeta_i(\alpha), \zeta_k(\alpha)\},\ i \neq k\ , 1 \leq i, k \leq N$. The total number of curves of this type is equal to any possible combination by pairs of the N viscous ratios, i.e. $\binom{N}{2} = N(N-1)/2$ curves.

Type II. Critical curves that relate pairs of different nonviscous ratios $\{\nu_i(\alpha), \nu_k(\alpha)\},\ i \neq k\ , 1 \leq i, k \leq N$. The total number of curves of this type is equal to any possible combination bypairs of the N nonviscous ratios, i.e. $\binom{N}{2} = N(N-1)/2$ curves.

Type III. Critical curves that relate the viscous and the nonviscous ratio of the ith kernel, $\{\zeta_i(\alpha), \nu_i(\alpha))\}\ , 1 \leq i \leq N$. The total number of curves of this type is equal to the number of kernels, N.

Type IV. Critical curves that relate the ith viscous ratio with the nonviscous ratio of the kth kernel, $\{\zeta_i(\alpha), \nu_k(\alpha)\},\ i \neq k\ , 1 \leq i, k \leq N$. For each ζ_i, $N-1$ different nonviscous ratios $\nu_k,\ 1 \leq k \leq N,\ k \neq i$. Hence, the total number is $N(N-1)$

Type I curves have already been determined above after solving for the unknowns ζ_i and ζ_k from Eqs. (26) and (27). In order to find curves of type II, it results much more suitable to address first the problem of determining R_i and R_k, considered as unknowns, solving later for ν_i and ν_k in a second step, using the relationship (25). Thus, after some straight manipulations, Eqs. (26) and (27) can be transformed into the two following second order polynomials in R_i and R_k, respectively.

$$\zeta_i(\zeta_i+\zeta_k)\,R_i^2(\alpha) - 2U_{ik}(\alpha)\,R_i(\alpha) + U_{ik}^2(\alpha) - \zeta_k V_{ik}(\alpha) = 0 \tag{33}$$

$$\zeta_k(\zeta_i+\zeta_k)\,R_k^2(\alpha) - 2U_{ik}(\alpha)\,R_k(\alpha) + U_{ik}^2(\alpha) - \zeta_i V_{ik}(\alpha) = 0 \tag{34}$$

whose roots are

$$R_i(\alpha) = \frac{U_{ik}(\alpha)}{\zeta_i+\zeta_k} \pm \frac{\sqrt{\Psi_{ik}(\alpha)}}{\zeta_i(\zeta_i+\zeta_k)} \tag{35}$$

$$R_k(\alpha) = \frac{U_{ik}(\alpha)}{\zeta_i+\zeta_k} \pm \frac{\sqrt{\Psi_{ik}(\alpha)}}{\zeta_k(\zeta_i+\zeta_k)} \tag{36}$$

TYPE I	$\{\zeta_i(\alpha), \zeta_k(\alpha)\}, \quad 0 < \alpha \leq 1, \;\; i \neq k, \;\; 1 \leq i, k \leq N$
Solution	$\zeta_i(\alpha) = \dfrac{R_k(\alpha)\, U_{ik}(\alpha) - V_{ik}(\alpha)}{R_i(\alpha)\,[R_k(\alpha) - R_i(\alpha)]}, \; \zeta_k(\alpha) = \dfrac{R_i(\alpha)\, U_{ik}(\alpha) - V_{ik}(\alpha)}{R_k(\alpha)\,[R_i(\alpha) - R_k(\alpha)]}$
(unique)	$U_{ik}(\alpha) = \dfrac{\alpha^2+1}{2\alpha} - \sum\limits_{\substack{j=1 \\ j\neq\{i,k\}}}^{N} R_j(\alpha)\,\zeta_j \;, \;\; V_{ik}(\alpha) = \dfrac{1}{\alpha} - \sum\limits_{\substack{j=1 \\ j\neq\{i,k\}}}^{N} R_j^2(\alpha)\,\zeta_j$
TYPE II	$\{\nu_i(\alpha), \nu_k(\alpha)\}, \quad 0 < \alpha \leq 1, \, i \neq k, \;\; 1 \leq i, k \leq N$
Solution (1)	$R_i(\alpha) = \dfrac{U_{ik}(\alpha)}{\zeta_i + \zeta_k} - \dfrac{\sqrt{\Psi_{ik}(\alpha)}}{\zeta_i(\zeta_i + \zeta_k)}, \; R_k(\alpha) = \dfrac{U_{ik}(\alpha)}{\zeta_i + \zeta_k} + \dfrac{\sqrt{\Psi_{ik}(\alpha)}}{\zeta_k(\zeta_i + \zeta_k)}$
Solution (2)	$R_i(\alpha) = \dfrac{U_{ik}(\alpha)}{\zeta_i + \zeta_k} + \dfrac{\sqrt{\Psi_{ik}(\alpha)}}{\zeta_i(\zeta_i + \zeta_k)}, \; R_k(\alpha) = \dfrac{U_{ik}(\alpha)}{\zeta_i + \zeta_k} - \dfrac{\sqrt{\Psi_{ik}(\alpha)}}{\zeta_k(\zeta_i + \zeta_k)}$
	$\Psi_{ik}(\alpha) = \zeta_i\,\zeta_k\left[(\zeta_i + \zeta_k)V_{ik}(\alpha) - U_{ik}^2(\alpha)\right]$
	$\nu_i(\alpha) = \alpha\dfrac{R_i(\alpha) - 1}{R_i(\alpha)} \;, \quad \nu_k(\alpha) = \alpha\dfrac{R_k(\alpha) - 1}{R_k(\alpha)}$
TYPE III	$\{\zeta_i(\alpha), \nu_i(\alpha)\}, \quad 0 < \alpha \leq 1, \, 1 \leq i \leq N$
Solution	$\zeta_i(\alpha) = \dfrac{U_i^2(\alpha)}{V_i(\alpha)}, \; R_i(\alpha) = \dfrac{V_i(\alpha)}{U_i(\alpha)}$
(unique)	$U_i(\alpha) = \dfrac{\alpha^2+1}{2\alpha} - \sum\limits_{\substack{j=1 \\ j\neq i}}^{N} R_j(\alpha)\,\zeta_j \;, \;\; V_i(\alpha) = \dfrac{1}{\alpha} - \sum\limits_{\substack{j=1 \\ j\neq i}}^{N} R_j^2(\alpha)\,\zeta_j$
	$\nu_i(\alpha) = \alpha\dfrac{R_i(\alpha) - 1}{R_i(\alpha)}$
TYPE IV	$\{\zeta_i(\alpha), \nu_k(\alpha)\}, \quad 0 < \alpha \leq 1, \, i \neq k, \;\; 1 \leq i, k \leq N$
Solution (1)	$\zeta_i(\alpha) = \dfrac{U_{ik}(\alpha)}{R_i(\alpha)} - \dfrac{\zeta_k}{2} + \dfrac{\sqrt{\zeta_k\,\Phi_{ik}(\alpha)}}{2R_i(\alpha)}, \; R_k(\alpha) = \dfrac{R_i(\alpha)}{2} - \dfrac{1}{2}\sqrt{\dfrac{\Phi_{ik}(\alpha)}{\zeta_k}}$
Solution (2)	$\zeta_i(\alpha) = \dfrac{U_{ik}(\alpha)}{R_i(\alpha)} - \dfrac{\zeta_k}{2} - \dfrac{\sqrt{\zeta_k\,\Phi_{ik}(\alpha)}}{2R_i(\alpha)}, \; R_k(\alpha) = \dfrac{R_i(\alpha)}{2} + \dfrac{1}{2}\sqrt{\dfrac{\Phi_{ik}(\alpha)}{\zeta_k}}$
	$\Phi_{ik}(\alpha) = R_i(\alpha)\,[R_i(\alpha)\zeta_k - 4U_{ik}(\alpha)] + 4V_{ik}(\alpha)$
	$\nu_k(\alpha) = \alpha\dfrac{R_k(\alpha) - 1}{R_k(\alpha)}$

Table 1: Closed-form expressions for the four types of critical curves

where

$$\Psi_{ik}(\alpha) = \zeta_i\,\zeta_k\left[(\zeta_i + \zeta_k)V_{ik}(\alpha) - U_{ik}^2(\alpha)\right] \tag{37}$$

Therefore, the final expressions of $\nu_i(\alpha)$ and $\nu_k(\alpha)$ are

$$\nu_i(\alpha) = \alpha - \frac{\alpha}{R_i(\alpha)} \;, \quad \nu_k(\alpha) = \alpha - \frac{\alpha}{R_k(\alpha)} \tag{38}$$

where here $R_i(\alpha)$ and $R_k(\alpha)$ come from Eqs. (35) and (36), respectively. In this case, the combination of the two pairs of solutions leads to two curves in parametric form. The union of these latter gives rise to the critical curves type II. A similar process can be carried out to derive type III and IV curves. A summary with the resulting closed-forms is presented in Table 1.

The formal definition of the critical parameter in the interval $0 < \alpha \leq 1$ has allowed to construct critical curves in parametric form. These results, shown in Table 1, constitute the main contributions of this paper. The interpretation of these analytical expressions should not be restricted only to plane curves, because they are closed-forms that depend not only on $\alpha \in (0, 1]$ but on more variables, specifically on the rest of

the damping ratios. From them, critical manifolds of larger dimension can also be determined in parametric form. Obviously, as the manifold dimension increases, it becomes more difficult to depict graphically.

From the Definition 4, a physical interpretation can be attributed to the critical parameter α. Indeed, along the graph of critical curves, that zone close to the left bound, $0 < \alpha \ll 1$ results in large critical eigenvalues (in absolute value), i.e. $|s| \gg \omega_n$. On the opposite side, values of α in a neighborhood around the right bound, $\alpha \approx 1$, lead to critical eigenvalues around the purely viscous critical value, i.e. $s \approx -\omega_n$.

As mentioned, critical curves relate every possible pair of damping parameters within the set $\boldsymbol{\theta} = \{\zeta_j, \nu_j\}_{j=1}^N$. Thus, a generic curve can be written using the following notation

$$\{\Theta_i(\alpha), \Theta_k(\alpha)\} \ , \quad 0 < \alpha \leq 1 \ , \ i \neq k \ , \quad \text{with } \Theta_i, \Theta_k \in \boldsymbol{\theta} = \{\zeta_1, \ldots, \zeta_N, \nu_1, \ldots, \nu_N\} \tag{39}$$

Before addressing the numerical validation of the above analytical expressions, a result that helps to relate the properties of critical curves and the nature of the associated critical eigenvalues will be proved.

Theorem 2. *Assume that* $\{\Theta_i(\alpha), \Theta_k(\alpha)\}$, $i \neq k$, $0 < \alpha \leq 1$ *represents any critical curve involving two damping parameters, where* $\Theta_i, \Theta_k \in \{\zeta_j, \nu_j\}_{j=1}^N$.

(i) If $\Theta_i'(\alpha) = 0$ *and* $\Theta_k'(\alpha) = 0$ *for some* $\alpha \in (0, 1]$, *then* $x = -1/\alpha$ *is a triple root of the equation* $\mathcal{D}(x) = 0$.

(ii) Inversely, if $x = -1/\alpha$ *is a triple root and*

$$\det \begin{bmatrix} \frac{\partial \mathcal{D}}{\partial \Theta_i} & \frac{\partial \mathcal{D}}{\partial \Theta_k} \\ \frac{\partial^2 \mathcal{D}}{\partial \Theta_i \partial x} & \frac{\partial^2 \mathcal{D}}{\partial \Theta_k \partial x} \end{bmatrix}_{x=-1/\alpha} \neq 0 \tag{40}$$

then $\Theta_i'(\alpha) = 0$ *and* $\Theta_k'(\alpha) = 0$, *where* $(\bullet)' = \partial(\bullet)/\partial\alpha$

Proof. (i) The graph $\{\Theta_i(\alpha), \Theta_k(\alpha)\}$, $0 < \alpha \leq 1$ draws a generic critical curve of any type (I, II, III or IV). Let us define the following single-variable functions

$$\mathcal{M}(\alpha) = \mathcal{D}(-1/\alpha)\Big|_{\Theta_i = \Theta_i(\alpha), \Theta_k = \Theta_k(\alpha)} = 0 \tag{41}$$

$$\mathcal{N}(\alpha) = \frac{\partial \mathcal{D}}{\partial x}\Big|_{x=-1/\alpha, \Theta_i = \Theta_i(\alpha), \Theta_k = \Theta_k(\alpha)} = 0 \ , \quad 0 < \alpha \leq 1 \tag{42}$$

The two equations $\mathcal{M}(\alpha) = 0$ and $\mathcal{N}(\alpha) = 0$ hold for every value of α within the interval $\alpha \in (0, 1]$. The derivatives $\Theta_i'(\alpha)$ and $\Theta_k'(\alpha)$ can be evaluated taking derivatives respect to α in both Eqs. (42) and using the chain rule.

$$\mathcal{M}'(\alpha) = \left[\frac{\partial \mathcal{D}}{\partial x}\left(\frac{1}{\alpha^2}\right) + \frac{\partial \mathcal{D}}{\partial \Theta_i}\Theta_i'(\alpha) + \frac{\partial \mathcal{D}}{\partial \Theta_k}\Theta_k'(\alpha)\right]_{x=-1/\alpha} = 0 \tag{43}$$

$$\mathcal{N}'(\alpha) = \left[\frac{\partial^2 \mathcal{D}}{\partial x^2}\left(\frac{1}{\alpha^2}\right) + \frac{\partial^2 \mathcal{D}}{\partial \Theta_i \partial x}\Theta_i'(\alpha) + \frac{\partial^2 \mathcal{D}}{\partial \Theta_k \partial x}\Theta_k'(\alpha)\right]_{x=-1/\alpha} = 0 \tag{44}$$

Let us assume that, for certain $\alpha_0 \in (0, 1]$, it is $\Theta_i'(\alpha_0) = \Theta_k'(\alpha_0) = 0$, then from Eq. (44) it yields

$$\frac{\partial^2 \mathcal{D}}{\partial x^2} = 0 \qquad \text{at } x_0 = -1/\alpha_0 \tag{45}$$

Since, additionally, it holds also that $\mathcal{D}(x_0) = \mathcal{D}'(x_0) = 0$, then it turns out that the critical eigenvalue $x_0 = -1/\alpha_0$ has multiplicity equal to 3 (it is a triple root).

(ii) Inversely, if $x = -1/\alpha$ is a triple root, then $\mathcal{D}(x) = \mathcal{D}'(x) = \mathcal{D}''(x) = 0$. Eqs (43) and (44) is then a homogeneous solvable system in $\Theta_i'(\alpha)$ and $\Theta_k'(\alpha)$, since the determinant, by hypothesis, is distinct of zero. The unique solution is therefore $\Theta_i'(\alpha) = \Theta_k'(\alpha) = 0$. □

Points which are simultaneously local extreme values of both $\Theta_i(\alpha)$ and $\Theta_k(\alpha)$ are easily identified along the graph of a critical curve because of their sharped and angled form (in fact, for them it is verified that $\Theta_i'(\alpha) = \Theta_k'(\alpha) = 0$). The Theorem 2 allows to relate such points with the multiplicity of critical eigenvalues. Thus, we will refer to them as *triple points*, since the characteristic equation associated to these damping parameters present a triple root (physically such root comes from the merging of the conjugate-complex pair and one of the N nonviscous eigenvalues). In the next Section, the numerical examples will enable validation the theoretical results derived above and in addition they will show that triple points can arise in general for all types of critical curves. Their number and shape will depend on the values adopted for the damping parameters, but invariably Theorem 2 will help us to identify them in graphical results.

4. Numerical examples

4.1. Revisiting the one-single-kernel based model

The determination of critical damping for single-degree-of-freedom oscillators with one single exponential kernel will be revisited in this point. The form and characteristics of this curve are already known in implicit form from the previous works of Adhikari [8, 10], Müler [9] and Muravyov [13]. Denoting just by $\zeta = \zeta_1$ and $\nu = \nu_1$ to the damping parameters of this model (avoiding subscripts), the dimensionless damping function in terms of $x = s/\omega_n$ yields

$$J(x) = \frac{G(x\,\omega_n)}{2m\omega_n} = \frac{\zeta}{1 + x\,\nu} \tag{46}$$

and. After deleting x from both equations $\mathcal{D}(x) = \mathcal{D}'(x) = 0$, the implicit expression of the critical curve can be written as [8]

$$8\zeta^3\nu + 12\zeta^2\nu^2 - \zeta^2 + 6\zeta\nu^3 - 10\zeta\nu + \nu^4 + 2\nu^2 + 1 = 0 \tag{47}$$

If explicit expressions of the form $\zeta(\nu)$ are required, they arise from the Cardano's formulas for a third order polynomial. As known [8], one of these roots can be discarded and the other two draw together two different pieces of the same curve in the plane (ζ, ν). Mathematically, the overdamped region is then defined as

$$\mathcal{OD} = \left\{(\zeta, \nu) \in \mathbb{R}^+ : \zeta_L(\nu) \leq \zeta \leq \zeta_U(\nu)\ ,\ 0 \leq \nu \leq 1/3\sqrt{3}\right\} \tag{48}$$

where the critical damping curves $\zeta_L(\nu)$, $\zeta_U(\nu)$ are

$$\begin{aligned} \zeta_L(\nu) &= \frac{1}{24\nu}\left[1 - 12\nu^2 + 2\sqrt{1 + 216\nu^2} + \cos\left(\frac{4\pi + \varphi(\nu)}{3}\right)\right] \\ \zeta_U(\nu) &= \frac{1}{24\nu}\left[1 - 12\nu^2 + 2\sqrt{1 + 216\nu^2} + \cos\left(\frac{\varphi(\nu)}{3}\right)\right] \end{aligned} \tag{49}$$

with

$$\varphi(\nu) = \arccos\left[-\frac{5832\nu^4 + 540\nu^2 - 1}{(1 + 216\nu^2)^{3/2}}\right] \tag{50}$$

Let us apply now the proposed method to determine the exact critical curve in parametric form: it corresponds to a type III curve and its closed-form expression can be read from Table 1, yielding

$$\zeta_c(\alpha) = \frac{\left(\alpha^2 + 1\right)^2}{4\alpha}\ ,\quad \nu_c(\alpha) = \frac{1}{2}\alpha\left(1 - \alpha^2\right)\ ,\quad 0 < \alpha \leq 1 \tag{51}$$

Both Eqs (47) and (51) represent the same curve but written in different forms. Furthermore, the set of points $(\nu, \zeta_L(\nu))$ and $(\nu, \zeta_U(\nu))$ are associated to two different subintervals in the range of α, say

$$\begin{aligned} \left\{(\nu, \zeta_U(\nu)) : 0 \leq \nu \leq 1/3\sqrt{3}\right\} &= \left\{(\nu_c(\alpha), \zeta_c(\alpha)) : 0 < \alpha \leq 1/\sqrt{3}\right\} \\ \left\{(\nu, \zeta_L(\nu)) : 0 \leq \nu \leq 1/3\sqrt{3}\right\} &= \left\{(\nu_c(\alpha), \zeta_c(\alpha)) : 1/\sqrt{3} \leq \alpha \leq 1\right\} \end{aligned} \tag{52}$$

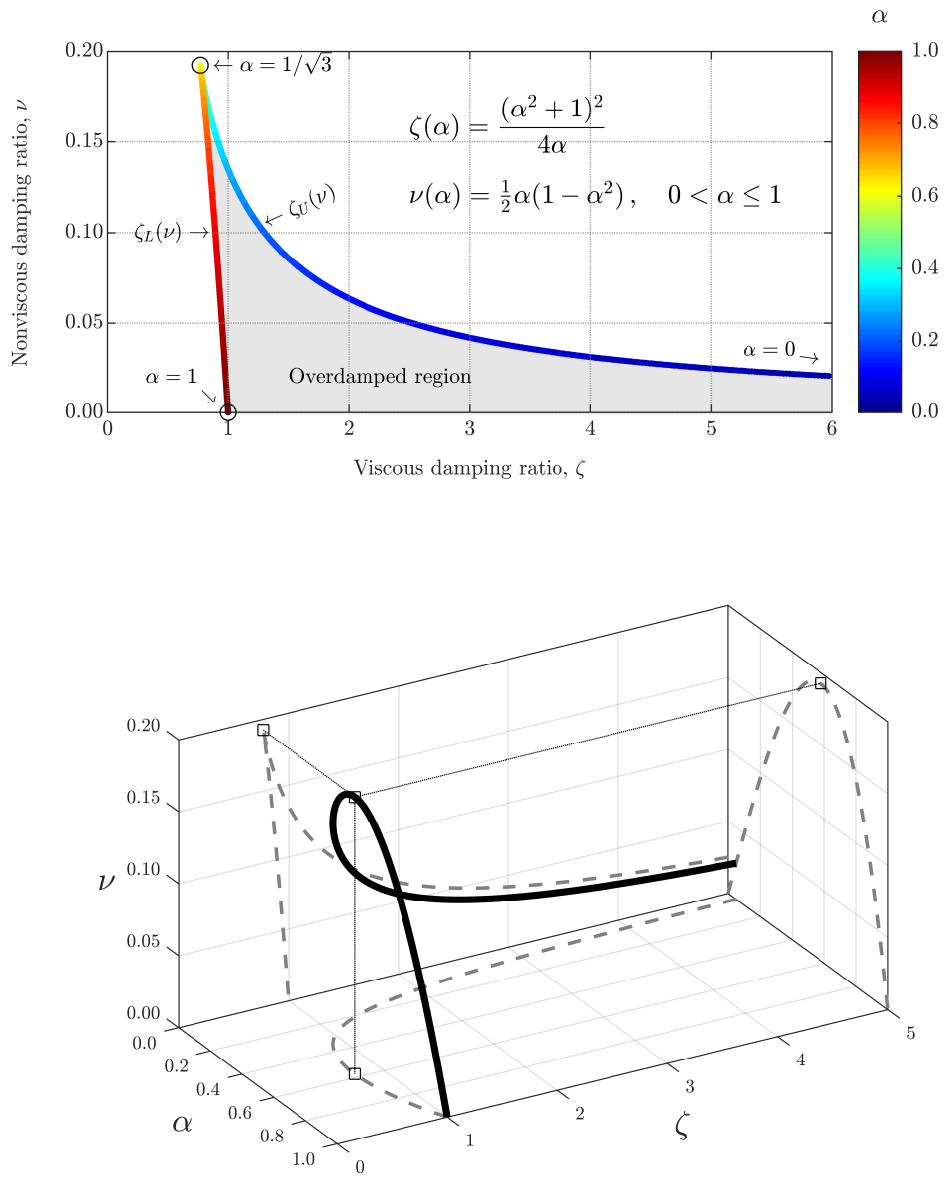

Figure 2: Top: Critical curve of the single-kernel nonviscous oscillator in plane (ζ, ν). The value of the critical parameter α is represented in scaled color along the curve. Bottom (black,"—"): Critical curve as a 3D parametric curve, $(\alpha, \zeta_c(\alpha), \nu_c(\alpha))$. Bottom (gray,"– –"): projections of the 3D-curve on each coordinate plane and location of the coordinates $(\alpha, \zeta, \nu) = (1, 4/3, 1/3)/\sqrt{3}$ associated to the triple eigenvalue $x = -\sqrt{3}$

The graph of the critical curve has been plotted in the Fig. 2(top) highlighting the actual value of the parameter $\alpha \in (0, 1]$ along the curve by means of scaled color. The display of the critical parameter allows to identify those zones of the curve where the critical eigenvalue $s = -\omega_n/\alpha$ becomes closer to the purely viscous behavior, i.e. $\alpha = 1$. In particular, according to Eqs. (51), the left and right endpoints $\alpha = \{0, 1\}$ leads to the edge points of the curve: $(\zeta, \nu) \to (\infty, 0)$ and $(\zeta, \nu) = (1, 0)$, respectively. In addition, it turns

out that curves $\zeta_L(\nu)$ and $\zeta_U(\nu)$ are associated mostly with $\alpha \approx 1$ and $\alpha \approx 0$, respectively. In Fig. 2(bottom) a 3D representation of the curve $(\alpha, \zeta_c(\alpha), \nu_c(\alpha)),\ 0 < \alpha \leq 1$ has been plotted together with the three projections of the curve over the three respective coordinate planes.

According to Theorem 2, candidates to be triple eigenvalues are those values of α which are simultaneously roots of $\zeta_c'(\alpha) = 0$ and $\nu_c(\alpha) = 0$. After some straight operations, two solutions are found: $\alpha = \pm 1/\sqrt{3}$. Evaluating the associated (nondimensonal) eigenvalues x and the damping parameters ζ and ν, yields

$$\begin{array}{llll} x = -\sqrt{3} & \zeta = 4/3\sqrt{3} & \nu = 1/3\sqrt{3} & \alpha = 1/\sqrt{3} \\ x = +\sqrt{3} & \zeta = -4/3\sqrt{3} & \nu = -1/3\sqrt{3} & \alpha = -1/\sqrt{3} \end{array} \tag{53}$$

Among the two found solutions, only the first one corresponds to a critical eigenvalue. For this case, the characteristic equation can be written as

$$\mathcal{D}(x) = x^2 + \frac{2x\zeta}{1 + x\nu} + 1 \tag{54}$$

If $\zeta = 4/3\sqrt{3}$ and $\nu = 1/3\sqrt{3}$, it is straightforward to verify that $x = -\sqrt{3}$ is root of the three following equations

$$\mathcal{D}(x) = 0\ , \quad \mathcal{D}'(x) = 0\ , \quad \mathcal{D}''(x) = 0 \tag{55}$$

concluding that it is a triple root, as predicted from the Theorem 2. The 3-tuple $(\alpha, \zeta, \nu) = (1, 4/3, 1/3)/\sqrt{3}$ has been depicted in the 3D plot of Fig. 2(bottom). Fig. 2(top) shows the critical curve in the coordinate axes (ζ, ν) as usually represented in the literature. The zone around the point $\zeta = 4/3\sqrt{3},\ \nu = 1/3\sqrt{3}$ is, from this point of view, sharpy and angled. However from a 3D perspective (Fig. 2,bottom), the 3D-curve $(\alpha, \zeta_c(\alpha), \nu_c(\alpha))$ manifests in fact quite smoothness at that point. The forthcoming examples will show that these points in general will be easily identified along the critical curves because in general coincide with a sharped zone of the critical curve and in addition they have the property of being local maximum or minimum points of the considered damping parameters.

4.2. Critical curves for multiple-kernel based models

In this example the main theoretical results will be validated for a nonviscous oscillator with three exponential hereditary kernels ($N = 3$). The above introduced dimensionless damping function can be written as

$$J(x) = \frac{G(s/\omega_n)}{2m\omega_n} = \frac{\zeta_1}{1 + x\,\nu_1} + \frac{\zeta_2}{1 + x\,\nu_2} + \frac{\zeta_3}{1 + x\,\nu_3} \tag{56}$$

The six damping parameters $\{\zeta_1, \zeta_2, \zeta_3, \nu_1, \nu_2, \nu_3\}$ can be combined in $N(2N-1) = 15$ pairs, which are making up the complete set of critical curves (1D-manifolds). However, as aforementioned, due to the symmetries of the parameters only 4 different curves can be distinguished. Without loss of generality, the following 4 critical curves will be considered: Type-I (ζ_1, ζ_2), Type-II (ν_1, ν_2), Type-III (ζ_1, ν_1) and Type-IV (ζ_1, ν_2); For each type of curve, different cases can be considered varying the remaining 4 parameters. In fact, as it will be seen later, the graphs can change drastically just modifying one these latter fixed parameters. It is not the objective of this work to study in detail their geometrical and topological behavior since considering all the possibilities would mean showing a huge number of graphs. Thus, four different examples (or cases) will be shown for each type. Table 2 lists the numerical values assumed for the fixed parameters together with the reference to the corresponding figure.

Critical curves type I (Fig. 3).

The graph of the critical curves can be drawn in the coordinate plane (ζ_1, ζ_2) considering the rest of the parameters fixed, i.e. $\zeta_3, \nu_1, \nu_2, \nu_3$. In the Table 2, four different cases, denoted by letters (a) to (d), have been considered. Along the curves, the scaled color shows graphically the value of the critical parameter α, and therefore an estimation of the actual critical eigenvalue $s = -\omega_n/\alpha$ can be predicted according to the color: from red $(\alpha = 1,\ s = -\omega_n)$ to blue $(\alpha = 0,\ s = -\infty)$. Figs. 3(a) and 3(b), show two plots for $\zeta_3 = 0$,

Figure(case)	Type	Variables	ζ_1	ζ_2	ζ_3	ν_1	ν_2	ν_3
3(a)	I	(ζ_1, ζ_2)	—	—	0.00	0.04	0.04	0.00
3(b)	I	(ζ_1, ζ_2)	—	—	0.00	0.01	0.06	0.00
3(c)	I	(ζ_1, ζ_2)	—	—	0.01	0.02	0.10	0.20
3(d)	I	(ζ_1, ζ_2)	—	—	0.04	0.02	0.10	0.35
4(a)	II	(ν_1, ν_2)	0.50	1.00	0.00	—	—	0.00
4(b)	II	(ν_1, ν_2)	1.20	1.20	0.00	—	—	0.00
4(c)	II	(ν_1, ν_2)	0.50	1.00	1.00	—	—	0.50
4(d)	II	(ν_1, ν_2)	0.50	0.50	2.00	—	—	0.01
5(a)	III	(ζ_1, ν_1)	—	0.20	0.00	—	0.05	0.00
5(b)	III	(ζ_1, ν_1)	—	0.10	0.80	—	0.05	0.01
5(c)	III	(ζ_1, ν_1)	—	0.60	1.00	—	0.10	0.02
5(d)	III	(ζ_1, ν_1)	—	0.80	1.10	—	0.10	0.01
6(a)	IV	(ζ_1, ν_2)	—	0.50	0.00	0.00	—	0.00
6(b)	IV	(ζ_1, ν_2)	—	4.00	0.00	0.01	—	0.00
6(c)	IV	(ζ_1, ν_2)	—	0.02	0.00	0.02	—	0.00
6(d)	IV	(ζ_1, ν_2)	—	0.10	0.02	0.01	—	0.10

Table 2: Numerical examples: distribution of the fixed damping parameters in the four considered type of critical curves. The symbol "—" makes reference to those parameters which are variables in the corresponding curve.

that is, assuming only two kernels. The first one —Fig. 3(a)— depicts the overdamped region when the two nonviscous ratios are equal: in this case $\nu_1 = \nu_2 = 0.04$. It is straightforward that in this case the damping function is reduced to that of the single-kernel oscillator

$$J(x) = \frac{\zeta_1 + \zeta_2}{1 + 0.04\, x} \tag{57}$$

The overdamped region (shaded) can easily be interpreted as the inequalities

$$\zeta_L(0.04) < \zeta_1 + \zeta_2 < \zeta_U(0.04)$$

where $\zeta_L(\nu)$ and $\zeta_U(\nu)$ are the lower and upper limits from Eq. (49) for single kernel oscillators' overdamped region. Thus, if $\nu_1 = \nu_2 > 1/3\sqrt{3}$, then the overdamped region would become the empty set. The second case —Fig. 3(b)— shows critical curves for distinct values of ν_1 and ν_2 ($\nu_1 \neq \nu_2$), arising new geometrical forms and in particular a triple point at $\zeta_1 \approx 13.7,\ \zeta_2 \approx 3.9$. In Figs. 3(c) and 3(d), the effect of adding a new kernel can be observed. Somehow, comparing Figs. 3(b) and 3(c), the overdamped region of two kernels is split up because of the new kernel, leading to two new disjoint overdamped regions. It turns out that both regions are disjoint within the positive range of the parameters, although considering also negative values of ζ_1 and ζ_2, it would be observed that in fact it is about the same region. It is just that they have common points in other quadrants. The gray shaded area emphasizes the overdamped region and it has been determined by identifying those points in the plane (ζ_1, ζ_2) which induce a completely overdamped motion. Thus, if for certain point (ζ_1, ζ_2), all the $2 + N = 5$ eigenvalues result to be real, then such point is plotted as a gray dot. Otherwise, it is not plotted. This construction therefore allows to validate the proposed methodology because in fact, the obtained critical curves fit perfectly to the gray region found by means of the above procedure.

Critical curves type II (Fig. 4).

Type II curves relate pairs of nonviscous ratios. In this example, the two first ratios (ν_1, ν_2) have been considered and the associated critical curves have been plotted in Fig. 4 in log scale for a better visualization. As before, it is suitable to graph the particular case with $N = 2$ kernels in order to interpret critical curves.

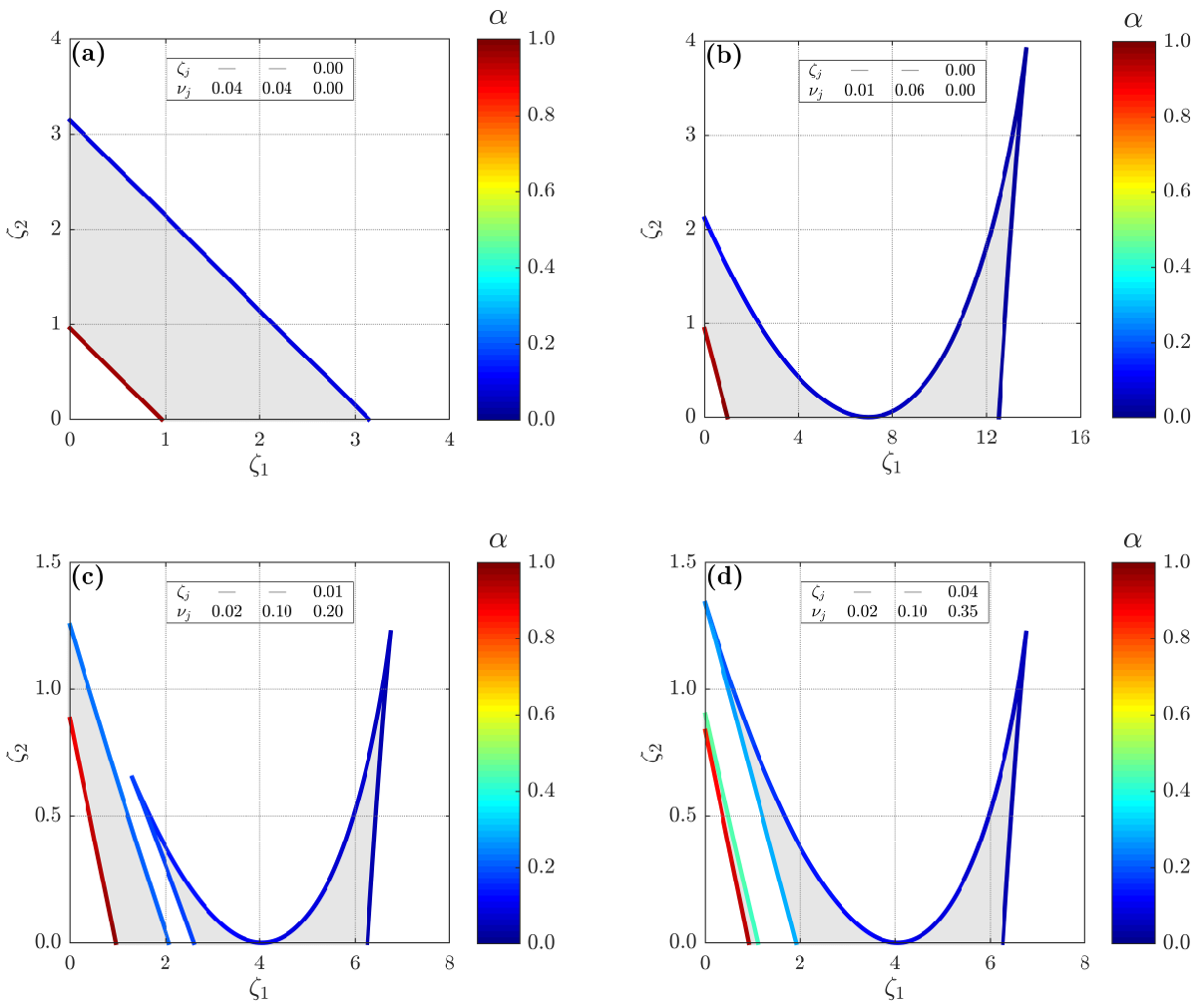

Figure 3: Type I critical curves of a nonviscous oscillator with $N = 3$ exponential kernels: Variable damping ratios: (ζ_1, ζ_2), fixed damping ratios: $(\zeta_3, \nu_1, \nu_2, \nu_3)$. The critical parameter α is depicted in scaled color along the curves

Figs. 4(a) and 4(b) show overdamped regions and critical curves for $\zeta_3 = 0$. The damping function for the particular case with $\zeta_1 = \zeta_2 = 1.20$ becomes

$$J(x) = 1.20 \left(\frac{1}{1 + x\,\nu_2} + \frac{1}{1 + x\,\nu_1} \right) \tag{58}$$

The model depicts symmetry respect to the variables ν_1 and ν_2, hence it is expected to have also symmetry of overdamped regions respect to the line $\nu_1 = \nu_2$ as indeed it occurs in Fig. 4(a). If the viscous damping ratios are distinct, $\zeta_1 \neq \zeta_2$, then the symmetry is broken and the presence of one, two or three disjoint overdamped regions will depend on the relative value of ζ_1 and ζ_2. For instance, Fig. 4(b) shows the case $\zeta_1 = 0.50,\ \zeta_2 = 1.00$ for which there are only two overdamped regions. In fact, searching for triple points (solving the three equations $\mathcal{D}(x) = \mathcal{D}'(x) = \mathcal{D}''(x) = 0$, we find just one at $\nu_1 \approx 2,\ \nu_2 \approx 0.15$. Figs. 4(c) and 4(d) shows the effect of adding a new kernel: for high values of ν_1 and ν_2, a new overdamped region linked to the new kernel appears. It can be observed that the higher the associated viscous damping ratio, ζ_3, the larger the size of the new right-top subregion.

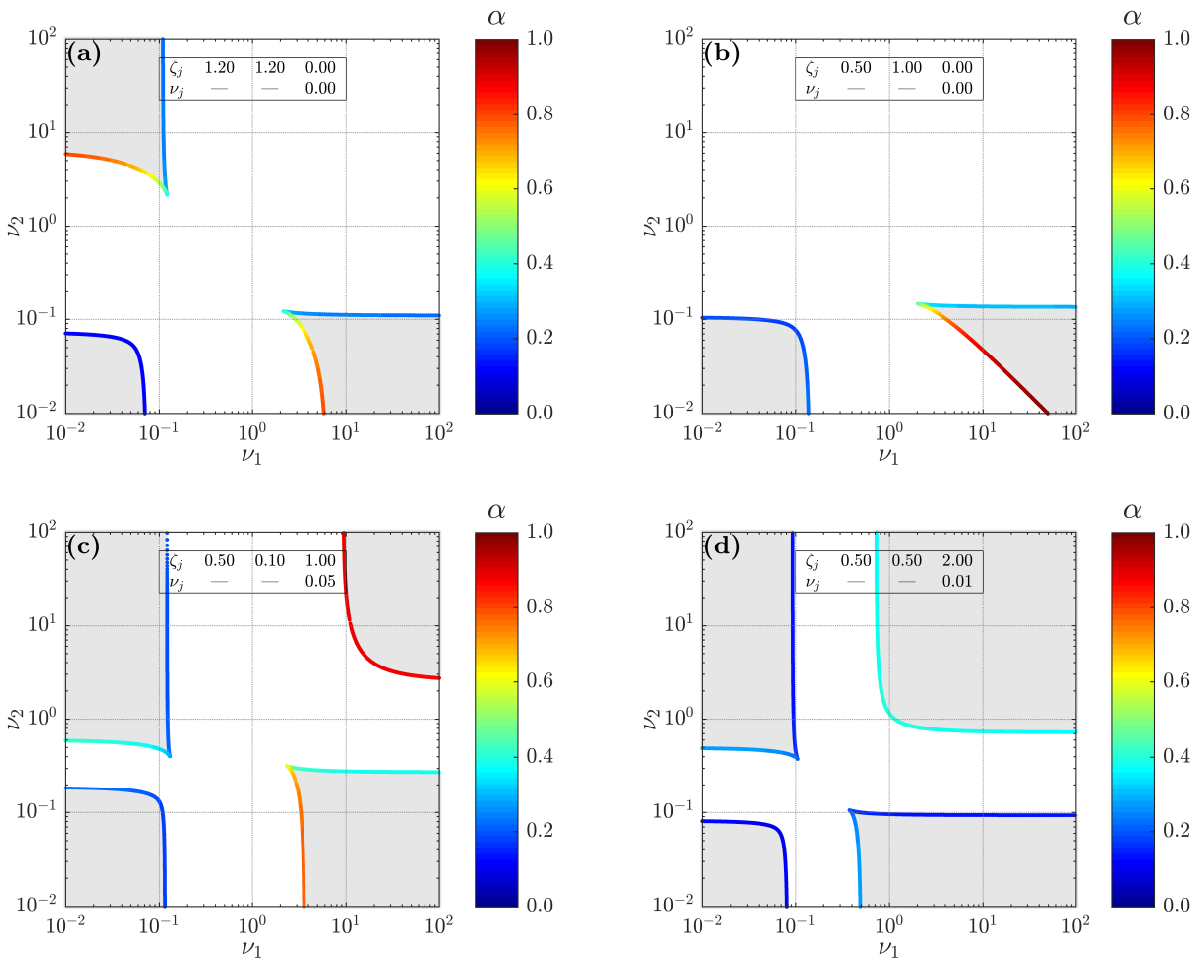

Figure 4: Type II critical curves of a nonviscous oscillator with $N = 3$ exponential kernels: Variable damping ratios: (ν_1, ν_2), fixed damping ratios: $(\zeta_1, \zeta_2, \zeta_3, \nu_3)$. The critical parameter α is depicted in scaled color along the curves. Overdamped regions are gray shaded

Critical curves type III (Fig. 5).

These curves are the critical relationships between both viscous and nonviscous ratios for each exponential kernel, i.e. (ζ_i, ν_i). They can be considered as extensions of that of the single-kernel model, obtained before. In fact, although in log-scale, certain similarities can be seen between the regions with form of "Δ" in Fig. 5(a) and 5(b) and that of Fig. 2. The main difference is due to the effect of the additional kernel: indeed, similarly to type I curves, the second kernel somehow divides the overdamped region into two disjointed regions. This outcome can be clearly visualized in Figs. 5(a) and 5(b), with two and three kernels respectively. The size of the overdamped regions seems to depend specially on the value of the viscous damping ratios.

Critical curves type IV (Fig. 6).

Finally, critical curves of type IV connect a viscous damping ratio with a nonviscous ratio from other kernel. Without loss of generality, in the current example the parameters (ζ_1, ν_2) have been chosen to depict such family of curves. The resulting graphs are expected to depend on the relative values of the rest of parameters ζ_2, ν_1 and, in addition, on the remaining kernels, say ζ_3, ν_3. Thus, differences between ζ_2 and

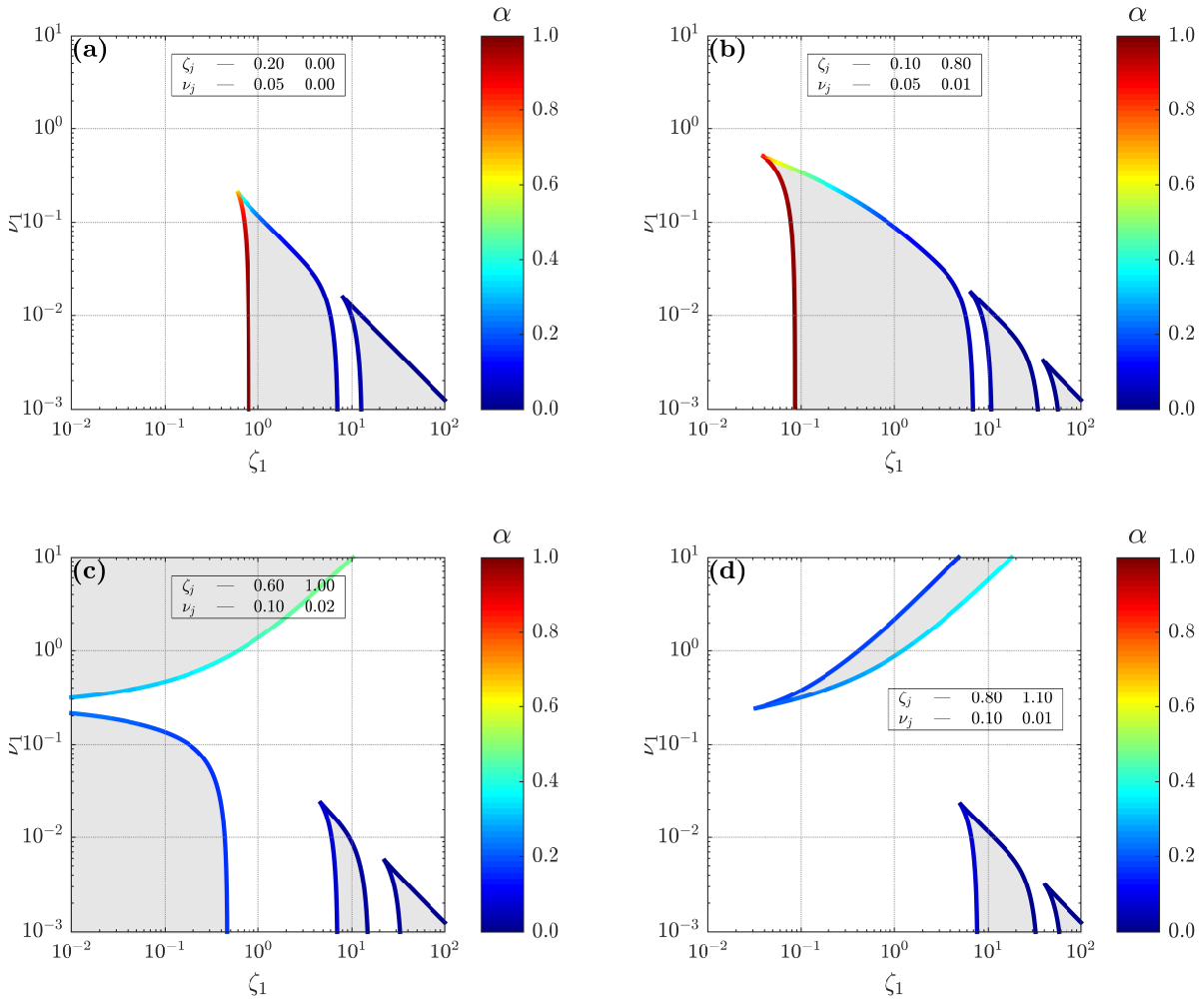

Figure 5: Type III critical curves of a nonviscous oscillator with $N = 3$ exponential kernels: Variable damping ratios: (ζ_1, ν_1), fixed damping ratios: $(\zeta_2, \zeta_3, \nu_2, \nu_3)$. The critical parameter α is depicted in scaled color along the curves. Overdamped regions are gray shaded

ν_1 can lead to significant changes in the geometric structure of the regions, as shown in Fig. 6(a), 6(b) and 6(c), built with just two kernels. If we also introduce another kernel with parameters $\zeta_3 = 0.02$ and $\nu_3 = 0.10$, —see Fig. 6(d)— the previous region is again split up in several disjoint overdamped regions, giving rise to two new triple points with the property of being local maximum or minimum of the curves $\zeta_1(\alpha)$ and $\nu_2(\alpha)$. In view of the graphical results (and in the absence of further study), it could also be concluded that, for the type IV curves, critical regions tend to concentrate in a band when the fixed viscous ratio ζ_2 is small, see Figs. 6(c) and 6(d).

The four types of critical curves have been represented for a numerical example with three exponential kernels. Although some patterns in the graphical behavior of the curves can be extrapolated, it becomes difficult to read and interpret the influence of the different parameters in the geometrical structure of the overdamped regions. Despite analytical tools to construct any critical curve are given, an *a-priori* prediction of the final shape in view of the value of the parameters is far from clear, being necessary the corresponding

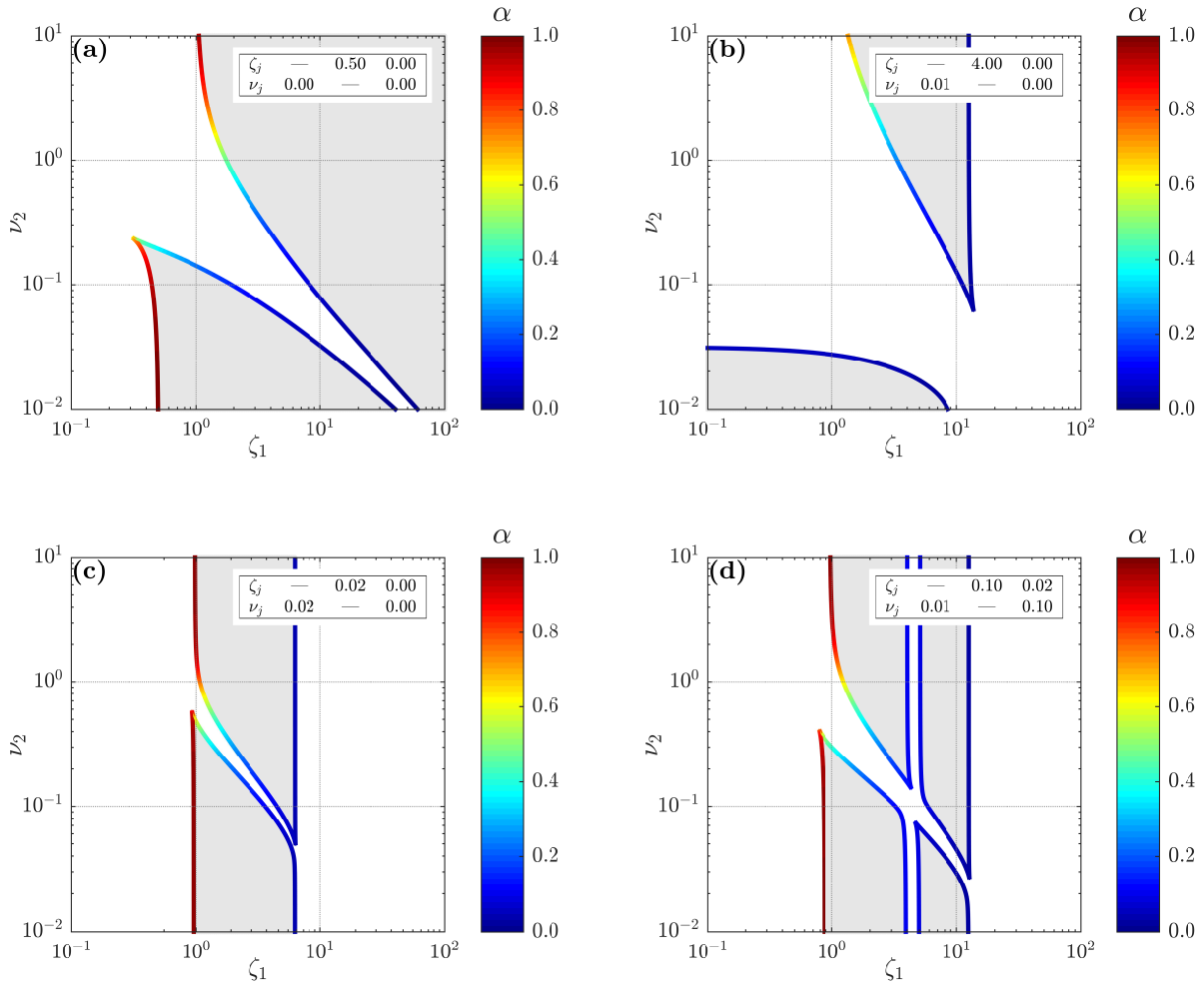

Figure 6: Type IV critical curves of a nonviscous oscillator with $N = 3$ exponential kernels: Variable damping ratios: (ζ_1, ν_2), fixed damping ratios: $(\zeta_2, \zeta_3, \nu_1, \nu_3)$. The critical parameter α is depicted in scaled color along the curves. Overdamped regions are gray shaded

graphical representation. This is perhaps a point to investigate in future works that could help to solve the inverse problem, which can be stated in the following terms: given a region in the damping space, what combinations of parameters allow to cover such a region?. In order to complete the numerical analysis, it is considered of interest to present also results of critical manifolds in 3D, that is, critical surfaces. This will be developed in the next example.

4.3. Critical surfaces for multiple-kernel based models

Putting another parameter into play and representing surfaces instead of curves enables us to visualize critical manifolds from a 3D point of view. The following example describes how to draw such critical surface in the 3D domain of three parameters, allowing us to interpret some of the above presented curves as simple cross sections. For that, a two-kernels model will be considered in which $\zeta_1 = \zeta_2 \equiv \zeta$. The nondimensional

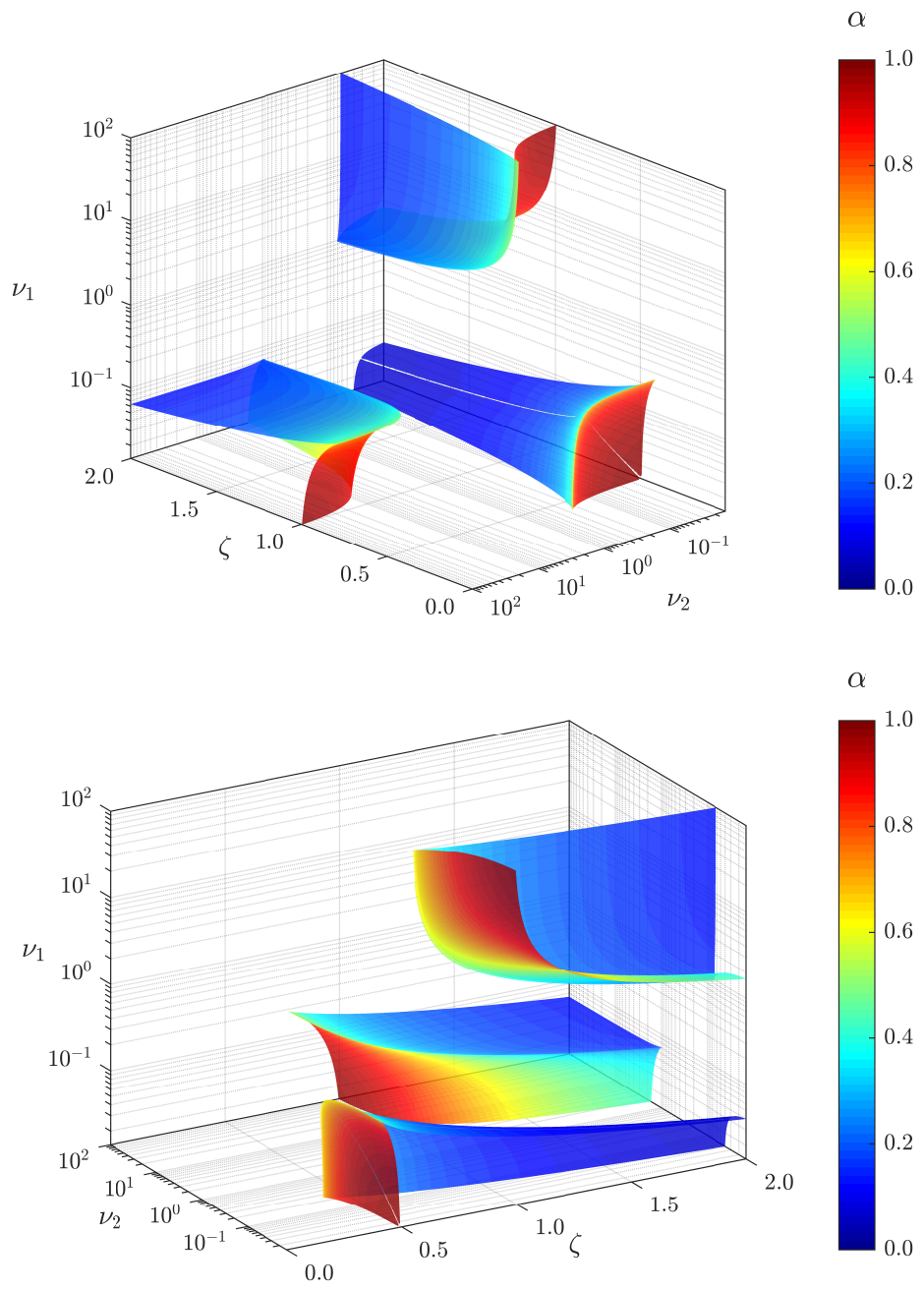

Figure 7: Critical surfaces in the space (ζ, ν_1, ν_2) for the two-kernels model with damping function $J(x) = \zeta/(1+x\,\nu_1)+\zeta/(1+x\,\nu_2)$. The scaled color on the surface represents the critical parameter α.

damping function yields then

$$J(x) = \zeta\left(\frac{1}{1+x\,\nu_1} + \frac{1}{1+x\,\nu_2}\right) \tag{59}$$

Equations $\mathcal{D}(x) = \mathcal{D}'(x) = 0$ can be solved in terms of ν_1 and ν_2 leading to critical curves of type II. Each function $\nu_1(\alpha)$ and $\nu_2(\alpha)$ depends in addition on the viscous damping ratio, ζ. Denoting this latter with other symbol, say β, these expressions can be rewritten highlighting their dependence on two variables, yielding then

$$\begin{cases} \zeta = \beta \\ \nu_1 = \nu_1(\alpha, \beta) \\ \nu_2 = \nu_2(\alpha, \beta) \ , \quad 0 < \alpha \leq 1 \ , \ 0 < \beta < \infty \end{cases} \tag{60}$$

where $\nu_1(\alpha, \beta)$ and $\nu_2(\alpha, \beta)$ are determined from the closed-forms provided in Table 1 (Type II, $N = 2$, $\zeta_1 = \zeta_2 = \beta$) The above three equations define a two-dimensional manifold in parametric form, i.e. a surface in the domain (ζ, ν_1, ν_2) which has been plotted in Fig. 7, using two points of view to a better interpretation. Cross sections of this figure lead to critical curves already described above. Thus, for instance, curves within the vertical plane $\zeta \equiv$ const can be identified in Fig. 4(a). Within cross sections of the form $\nu_2 \equiv$ const $\ll 1$, two overdamped regions can be distinguished. These latter can also be observed in Fig. 6(a). If, on the contrary, we take cutting planes with $\nu_2 \equiv$ const $\gg 1$, the effect of the second kernel disappears and remains the typical overdamped region of a single-kernel model, see Fig. 2(top).

The presence of triple points is also noticeable when observing critical surfaces in a 3D space. While those ones were identified as simple points on the plane, they now emerge as curves in space. Indeed, it is possible to solve from the three equations $\mathcal{D}(x) = \mathcal{D}'(x) = \mathcal{D}''(x) = 0$ the three unknowns $\zeta(\alpha)$, $\nu_1(\alpha)$ and $\nu_2(\alpha)$, as a function of the critical parameter, giving rise to a spatial curve. These curves can be clearly noticed in Fig. 7 as the union of a family of local maximums or minimums of critical curves.

Finally, the critical surfaces have also been colored using the same scale as the previous examples. Those critical eigenvalues closer to the viscous behavior ($\alpha \approx 1$, $s \approx -\omega_n$) are mainly concentrated for those lowest values of the damping ratio, ζ. Somehow, the bigger the viscous ratio ζ, the more negative the critical eigenvalue (in terms of the critical parameter it is $\alpha \ll 1$, characteristic of blue color zones).

According to the results given above for type II curves, the hypothetical presence of different viscous ratios, i.e. $\zeta_1 \neq \zeta_2$, would result in a non-symmetric reorganization of the two shells observed in Fig. 7, the first one in the region $\nu_1 \ll 1, \nu_2 \gg 1$ and the second one for $\nu_1 \gg 1, \nu_2 \ll 1$.

As it has been seen, critical manifolds of one dimension (curves) represent boundaries between overdamped 2D-regions (gray shaded in the Figs. 3 to 6). Critical manifolds of two dimensions (surfaces) represent in turn thresholds between overdamped 3D-regions (volumes, although the have not been highlighted in Fig. 7). The next step would seem to be the representation of 3D manifolds, i.e. volumes, although theoretically they are boundaries of 4D overdamped regions. Obviously, this representation is not very intuitive and it becomes difficult to interpret; perhaps dynamic graphics could help, but it would require a great deal of abstraction to identify the meaning of such moving volumes. For that reason, in this article at most critical surfaces have been covered (from a graphical point of view), leaving for future publications new possible geometrical manifestations that allow to visualize critical manifolds of higher dimensions. In any case, we consider that the fundamental objective of the article has been achieved, since the developed methodology is theoretically exact and consistent, allowing to solve any critical manifold in parametric form. Just as it has been commented previously, the question of the inverse problem now arises: given certain overdamped region, what damping parameters generate it? This approach could be of great interest for the design processes of viscoelastic materials. The challenge for future works is to extend this methodology for multiple degrees of freedom nonviscous systems with multiple exponential kernels, something that is currently been carried out.

5. Conclusions

In this paper, multiple-kernel based single degree-of-freedom viscoelastic oscillators have been considered. Nonviscous or viscoelastic vibrating structures present dissipative forces depending on the past history of the velocity response via convolution integrals over hereditary exponential kernels. In this paper, the number

of exponential kernel does not suppose any limitation and the derivations have been carried out considering any number $N \geq 1$. It is known that the oscillatory nature of the response depends on the eigenvalues of the system in the frequency domain. If the system is lightly damped the set of eigenvalues is formed a pair of conjugate-complex pair and N different nonviscous eigenvalues. But, under certain conditions of damping, the conjugate-complex pair can merge into the real axis and be transformed into real eigenvalues. In this paper, the set of damping parameters are considered as dependent variables. In such domain, the thresholds between oscillatory and non–oscillatory induced motion are called critical manifolds (curves or surfaces for particular cases of 1D and 2D dimensional manifolds).

Previous works have demonstrated that the critical curves in implicit form emerge from eliminating the Laplace parameter s from the characteristic equation and from its s-derivative. This methodology can not be carried out if $N \geq 4$ because the resulting polynomial has consequently a degree higher than 5, something that impedes its solution by radicals. In this paper, a new method to determine exactly closed-forms of critical manifolds is proposed. The procedure is based on changing the perspective over the Laplace parameter s; instead of identifying it as an unknown, we propose to read it as a variable parameter. Some theoretical results demonstrate the suitability of such parameter, which is redefined in dimensionless form. As consequence, closed-form analytical expressions of every type of critical curves have been derived. The so-determined critical manifolds have been validated through numerical examples, in which critical curves and critical surfaces have been represented. Since the developed approach is analytical, the representation of the obtained expressions fit exactly with the numerically determined overdamped regions.

References

[1] D. Golla, P. Hughes, Dynamics of viscoelastic structures - a time-domain, finite-element formulation, Journal of Applied Mechanics-Transactions of the ASME 52 (4) (1985) 897–906.

[2] N. Wagner, S. Adhikari, Symmetric state-space method for a class of nonviscously damped systems, AIAA Journal 41 (5) (2003) 951–956.

[3] M. Biot, Variational principles in irreversible thermodynamics with application to viscoelasticity, Physical Review 97 (6) (1955) 1463–1469.

[4] M. Lázaro, Nonviscous modes of nonproportionally damped viscoelastic systems, Journal of Applied Mechanics (Transactions of ASME) 82 (12) (2015) Art. 121011 (9 pp).

[5] S. Mohammadi, H. Voss, Variational characterization of real eigenvalues in linear viscoelastic oscillators, Mathematics and Mechanics of Solids 23 (10) (2018) 1377–1388, cited By 2. doi:10.1177/1081286517726368.

[6] S. Mohammadi, H. Voss, On the distribution of real eigenvalues in linear viscoelastic oscillators, Numerical Linear Algebra with ApplicationsCited By 0; Article in Press. doi:10.1002/nla.2228.

[7] A. Muravyov, Forced vibration responses of viscoelastic structure, Journal of Sound and Vibration 218 (5) (1998) 892–907.

[8] S. Adhikari, Qualitative dynamic characteristics of a non-viscously damped oscillator, Proceedings of the Royal Society A-Mathematical Physical and Engineering Sciences 461 (2059) (2005) 2269–2288.

[9] P. Muller, Are the eigensolutions of a l-d.o.f. system with viscoelastic damping oscillatory or not?, Journal of Sound and Vibration 285 (1-2) (2005) 501–509.

[10] S. Adhikari, Dynamic response characteristics of a nonviscously damped oscillator, Journal of Applied Mechanics-Transactions of the ASME 75 (1) (2008) 011003.01–011003.12.

[11] M. Lázaro, Critical damping in non-viscously damped linear systems, Applied Mathematical Modelling 65 (2019) 661–675.

[12] C. Bert, Material Damping - Introductory Review Of Mathematical-models, Measures And Experimental Techniques, Journal of Sound and Vibration 29 (2) (1973) 129–153.

[13] A. Muravyov, S. Hutton, Free vibration response characteristics of a simple elasto-hereditary system, Journal of Vibration and Acoustics-Transactions of the ASME 120 (2) (1998) 628–632.